

Geometric Nonlinear PID Control of a Quadrotor UAV on $SE(3)$

Farhad Goodarzi, Daewon Lee, and Taeyoung Lee*

Abstract—Nonlinear PID control systems for a quadrotor UAV are proposed to follow an attitude tracking command and a position tracking command. The control systems are developed directly on the special Euclidean group to avoid singularities of minimal attitude representations or ambiguity of quaternions. A new form of integral control terms is proposed to guarantee almost global asymptotic stability when there exist uncertainties in the quadrotor dynamics. A rigorous mathematical proof is given. Numerical example illustrating a complex maneuver, and a preliminary experimental result are provided.

I. INTRODUCTION

A quadrotor unmanned aerial vehicle (UAV) has been envisaged for various applications such as surveillance, sensing or educational purposes, due to its ability to hover with simpler mechanical structures compared to helicopters. Several control systems have been developed based on backstepping, sliding mode controller, or adaptive neural network [1], [2], [3]. Aggressive maneuvers are also demonstrated at [4]. However, these are based on Euler angles. Therefore they involve complicated expressions for trigonometric functions, and they exhibit singularities which restrict their ability to achieve complex rotational maneuvers significantly.

There are quadrotor control systems developed in terms of quaternions [5]. Quaternions do not have singularities but, as the three-sphere double-covers the special orthogonal group, one attitude may be represented by two antipodal points on the three-sphere. This ambiguity should be carefully resolved in quaternion-based attitude control systems, otherwise they may exhibit unwinding, where a rigid body unnecessarily rotates through a large angle even if the initial attitude error is small [6]. To avoid these, an additional mechanism to lift attitude onto the unit-quaternion space is introduced [7].

There are other limitations of quadrotor control systems such as complexities in controller structures or lack of stability proof. For example, tracking control of a quadrotor UAV has been considered in [8], [9], but the control system in [8] has a complex structure since it is based on a multiple-loop backstepping approach, and no stability proof is presented in [9]. Robust tracking control systems are studied in [10], [11], but the quadrotor dynamics is simplified by considering planar motion only [10], or by ignoring the rotational dynamics by timescale separation assumption [11].

Recently, the dynamics of a quadrotor UAV is globally expressed on the special Euclidean group, $SE(3)$, and nonlinear control systems are developed to track outputs

of several flight modes [12]. Several aggressive maneuvers of a quadrotor UAV are demonstrated based on a hybrid control architecture, and a nonlinear robust control system is also considered in [13]. As they are directly developed on the special Euclidean group, complexities, singularities, and ambiguities associated with minimal attitude representations or quaternions are completely avoided [14].

This paper is an extension of the prior works of the author in [12], [13]. It is assumed that there exist uncertainties on the translational dynamics and the rotational dynamics of a quadrotor UAV, and nonlinear PID controllers are proposed to follow an attitude tracking command and a position tracking command. Linear or nonlinear PID controllers have been widely used in various experimental settings for a quadrotor UAV, without careful stability analyses. This paper provides a new form of integral control terms that guarantees asymptotic convergence of tracking errors with uncertainties. The nonlinear robust tracking control system in [13] provides ultimate boundedness of tracking errors, and the control input may be prone to chattering if the required ultimate bound is smaller. Compared with [13], the control system in this paper provides stronger asymptotic stability, and there is no concern for discontinuities. The structure of the control system is also simplified such that the cross term of the angular velocity does not have to be cancelled.

In short, the unique features of the control system proposed in this paper are as follows: (i) it is developed for the full six degrees of freedom dynamic model of a quadrotor UAV on $SE(3)$, including the coupling between the translational dynamics and the rotational dynamics, (ii) a rigorous Lyapunov analysis is presented to establish stability properties without any timescale separation assumption, and (iii) it is guaranteed to be robust against unstructured uncertainties in both the translational dynamics and the rotational dynamics, (iv) in contrast to hybrid control systems [15], complicated reachability set analysis is not required to guarantee safe switching between different flight modes, as the region of attraction for each flight mode covers the configuration space almost globally. To the author's best knowledge, a rigorous mathematical analysis of nonlinear PID-like controllers of a quadrotor UAV with almost global asymptotic stability on $SE(3)$ has been unprecedented.

II. QUADROTOR DYNAMICS MODEL

Consider a quadrotor UAV model illustrated in Figure 1. We choose an inertial reference frame $\{\vec{e}_1, \vec{e}_2, \vec{e}_3\}$ and a body-fixed frame $\{\vec{b}_1, \vec{b}_2, \vec{b}_3\}$. The origin of the body-fixed frame is located at the center of mass of this vehicle. The

Farhad Goodarzi, Daewon Lee, Taeyoung Lee, Mechanical and Aerospace Engineering, The George Washington University, Washington DC 20052 {fgoodarzi, daewonlee, tylee}@gwu.edu

*This research has been supported in part by NSF under the grant CMMI-1243000 (transferred from 1029551).

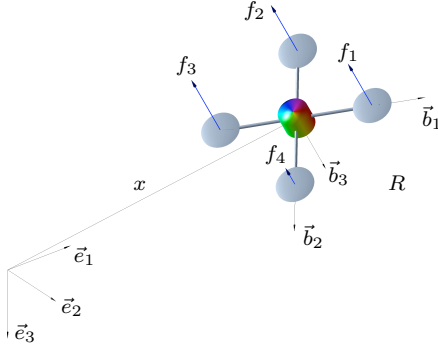


Fig. 1. Quadrotor model

first and the second axes of the body-fixed frame, \vec{b}_1, \vec{b}_2 , lie in the plane defined by the centers of the four rotors.

The configuration of this quadrotor UAV is defined by the location of the center of mass and the attitude with respect to the inertial frame. Therefore, the configuration manifold is the special Euclidean group $SE(3)$, which is the semidirect product of \mathbb{R}^3 and the special orthogonal group $SO(3) = \{R \in \mathbb{R}^{3 \times 3} \mid R^T R = I, \det R = 1\}$.

The mass and the inertial matrix of a quadrotor UAV are denoted by $m \in \mathbb{R}$ and $J \in \mathbb{R}^{3 \times 3}$. Its attitude, angular velocity, position, and velocity are defined by $R \in SO(3)$, $\Omega, x, v \in \mathbb{R}^3$, respectively, where the rotation matrix R represents the linear transformation of a vector from the body-fixed frame to the inertial frame and the angular velocity Ω is represented with respect to the body-fixed frame. The distance between the center of mass to the center of each rotor is $d \in \mathbb{R}$, and the i -th rotor generates a thrust f_i and a reaction torque τ_i along $-\vec{b}_3$ for $1 \leq i \leq 4$. The magnitude of the total thrust and the total moment in the body-fixed frame are denoted by $f, M \in \mathbb{R}^3$, respectively.

The following conventions are assumed for the rotors and propellers, and the thrust and moment that they exert on the quadrotor UAV. We assume that the thrust of each propeller is directly controlled, and the direction of the thrust of each propeller is normal to the quadrotor plane. The first and third propellers are assumed to generate a thrust along the direction of $-\vec{b}_3$ when rotating clockwise; the second and fourth propellers are assumed to generate a thrust along the same direction of $-\vec{b}_3$ when rotating counterclockwise. Thus, the thrust magnitude is $f = \sum_{i=1}^4 f_i$, and it is positive when the total thrust vector acts along $-\vec{b}_3$, and it is negative when the total thrust vector acts along \vec{b}_3 . By the definition of the rotation matrix $R \in SO(3)$, the total thrust vector is given by $-fRe_3 \in \mathbb{R}^3$ in the inertial frame. We also assume that the torque generated by each propeller is directly proportional to its thrust. Since it is assumed that the first and the third propellers rotate clockwise and the second and the fourth propellers rotate counterclockwise to generate a positive thrust along the direction of $-\vec{b}_3$, the torque generated by the i -th propeller about \vec{b}_3 can be written as $\tau_i = (-1)^i c_{\tau f} f_i$ for a fixed constant $c_{\tau f}$. All of these assumptions are fairly common in many quadrotor control systems [5], [16].

Under these assumptions, the thrust of each propeller

f_1, f_2, f_3, f_4 is directly converted into f and M , or vice versa. In this paper, the thrust magnitude $f \in \mathbb{R}$ and the moment vector $M \in \mathbb{R}^3$ are viewed as control inputs. The equations of motion are given by

$$\dot{x} = v, \quad (1)$$

$$m\dot{v} = mge_3 - fRe_3 + \Delta_x, \quad (2)$$

$$\dot{R} = R\hat{\Omega}, \quad (3)$$

$$J\dot{\Omega} + \Omega \times J\Omega = M + \Delta_R, \quad (4)$$

where the *hat map* $\hat{\cdot} : \mathbb{R}^3 \rightarrow \mathfrak{so}(3)$ is defined by the condition that $\hat{x}y = x \times y$ for all $x, y \in \mathbb{R}^3$. This identifies the Lie algebra $\mathfrak{so}(3)$ with \mathbb{R}^3 using the vector cross product in \mathbb{R}^3 . The inverse of the hat map is denoted by the *vee* map, $\vee : \mathfrak{so}(3) \rightarrow \mathbb{R}^3$. Unstructured, but fixed uncertainties in the translational dynamics and the rotational dynamics of a quadrotor UAV are denoted by Δ_x and $\Delta_R \in \mathbb{R}^3$, respectively.

Throughout this paper, $\lambda_m(A)$ and $\lambda_M(A)$ denote the minimum eigenvalue and the maximum eigenvalue of a square matrix A , respectively, and λ_m and λ_M are shorthand for $\lambda_m = \lambda_m(J)$ and $\lambda_M = \lambda_M(J)$. The two-norm of a matrix A is denoted by $\|A\|$.

III. ATTITUDE CONTROLLED FLIGHT MODE

Since the quadrotor UAV has four inputs, it is possible to achieve asymptotic output tracking for at most four quadrotor UAV outputs. The quadrotor UAV has three translational and three rotational degrees of freedom; it is not possible to achieve asymptotic output tracking of both attitude and position of the quadrotor UAV. This motivates us to introduce two flight modes, namely (1) an attitude controlled flight mode, and (2) a position controlled flight mode. While a quadrotor UAV is underactuated, a complex flight maneuver can be defined by specifying a concatenation of flight modes together with conditions for switching between them. This will be further illustrated by a numerical example later. In this section, an attitude controlled flight mode is considered.

A. Attitude Tracking Errors

Suppose that an smooth attitude command $R_d(t) \in SO(3)$ satisfying the following kinematic equation is given:

$$\dot{R}_d = R_d\hat{\Omega}_d, \quad (5)$$

where $\Omega_d(t)$ is the desired angular velocity, which is assumed to be uniformly bounded. We first define errors associated with the attitude dynamics as follows [17], [18].

Proposition 1: For a given tracking command (R_d, Ω_d) , and the current attitude and angular velocity (R, Ω) , we define an attitude error function $\Psi : SO(3) \times SO(3) \rightarrow \mathbb{R}$, an attitude error vector $e_R \in \mathbb{R}^3$, and an angular velocity error vector $e_\Omega \in \mathbb{R}^3$ as follows:

$$\Psi(R, R_d) = \frac{1}{2} \text{tr}[I - R_d^T R], \quad (6)$$

$$e_R = \frac{1}{2} (R_d^T R - R^T R_d)^\vee, \quad (7)$$

$$e_\Omega = \Omega - R^T R_d \Omega_d, \quad (8)$$

Then, the following properties hold:

- (i) Ψ is positive-definite about $R = R_d$.
- (ii) The left-trivialized derivative of Ψ is given by

$$\mathbf{T}_I^* \mathbf{L}_R(\mathbf{D}_R \Psi(R, R_d)) = e_R. \quad (9)$$

- (iii) The critical points of Ψ , where $e_R = 0$, are $\{R_d\} \cup \{R_d \exp(\pi \hat{s}), s \in \mathbb{S}^2\}$.
- (iv) A lower bound of Ψ is given as follows:

$$\frac{1}{2} \|e_R\|^2 \leq \Psi(R, R_d), \quad (10)$$

- (v) Let ψ be a positive constant that is strictly less than 2. If $\Psi(R, R_d) < \psi < 2$, then an upper bound of Ψ is given by

$$\Psi(R, R_d) \leq \frac{1}{2 - \psi} \|e_R\|^2. \quad (11)$$

- (vi) The time-derivative of Ψ and e_R satisfies:

$$\dot{\Psi} = e_R \cdot e_\Omega, \quad \|\dot{e}_R\| \leq \|e_\Omega\|. \quad (12)$$

Proof: See [18]. ■

B. Attitude Tracking Controller

We now introduce a nonlinear controller for the attitude controlled flight mode:

$$M = -k_R e_R - k_\Omega e_\Omega - k_I e_I + (R^T R_d \Omega_d)^\wedge J R^T R_d \Omega_d + J R^T R_d \dot{\Omega}_d, \quad (13)$$

$$e_I = \int_0^t e_\Omega(\tau) + c_2 e_R(\tau) d\tau, \quad (14)$$

where k_R, k_Ω, k_I, c_2 are positive constants. The control moment is composed of proportional, derivative, and integral terms, augmented with additional terms to cancel out the angular acceleration caused by the desired angular velocity. One noticeable difference from the attitude control systems in [12], [13] is that the cross term at (4), namely $\Omega \times J \Omega$ does not have to be cancelled. This simplifies controller structures.

Unlike common integral control terms where the attitude error is integrated only, here the angular velocity error is also integrated at (14). This unique term is required to show exponential stability in the presence of the disturbance Δ_R in the subsequent analysis. From (12), it essentially increases the proportional term. The corresponding effective controller gains for the proportional term and the integral term are given by $k_R + k_I$ and $c_2 k_I$, respectively. We now state the result that the zero equilibrium of tracking errors (e_R, e_Ω) is exponentially stable.

Proposition 2: (Attitude Controlled Flight Mode) Consider the control moment M defined in (13)-(14). For positive constants k_R, k_Ω , the constants c_2, B_2 are chosen such that

$$\|(2J - \text{tr}[J]I)\| \|\Omega_d\| \leq B_2, \quad (15)$$

$$c_2 < \min \left\{ \frac{\sqrt{k_R \lambda_m}}{\lambda_M}, \frac{4k_\Omega}{8k_R \lambda_M + (k_\Omega + B_2)^2} \right\}, \quad (16)$$

Then, the equilibrium of the zero attitude tracking errors $(e_R, e_\Omega, e_I) = (0, 0, \frac{\Delta_R}{k_I})$ is almost globally asymptotically

stable with respect to e_R and e_Ω ¹, and the integral term e_I is globally uniformly bounded. It is also locally exponentially stable with respect to e_R and e_Ω .

Proof: See Appendix A. ■

While these results are developed for the attitude dynamics of a quadrotor UAV, they can be applied to the attitude dynamics of any rigid body. Nonlinear PID-like controllers have been developed for attitude stabilization in terms of modified Rodriguez parameters [20] and quaternions [21], and for attitude tracking in terms of Euler-angles [22]. The proposed tracking control system is developed on $\text{SO}(3)$, therefore it avoids singularities of Euler-angles and Rodriguez parameters, as well as unwinding of quaternions.

Asymptotic tracking of the quadrotor attitude does not require specification of the thrust magnitude. As an auxiliary problem, the thrust magnitude can be chosen in many different ways to achieve an additional translational motion objective. For example, it can be used to asymptotically track a quadrotor altitude command [23]. Since the translational motion of the quadrotor UAV can only be partially controlled; this flight mode is most suitable for short time periods where an attitude maneuver is to be completed.

IV. POSITION CONTROLLED FLIGHT MODE

We now introduce a nonlinear controller for the position controlled flight mode.

A. Position Tracking Errors

Suppose that an arbitrary smooth position tracking command $x_d(t) \in \mathbb{R}^3$ is given. The position tracking errors for the position and the velocity are given by:

$$e_x = x - x_d, \quad e_v = \dot{e}_x = v - \dot{x}_d. \quad (17)$$

Similar with (14), an integral control term for the position tracking controller is defined as

$$e_i = \int_0^t e_v(\tau) + c_1 e_x(\tau) d\tau, \quad (18)$$

for a positive constant c_1 specified later.

For a positive constant $\sigma \in \mathbb{R}$, a saturation function $\text{sat}_\sigma : \mathbb{R} \rightarrow [-\sigma, \sigma]$ is introduced as

$$\text{sat}_\sigma(y) = \begin{cases} \sigma & \text{if } y > \sigma \\ y & \text{if } -\sigma \leq y \leq \sigma \\ -\sigma & \text{if } y < -\sigma \end{cases}.$$

If the input is a vector $y \in \mathbb{R}^n$, then the above saturation function is applied element by element to define a saturation function $\text{sat}_\sigma(y) : \mathbb{R}^n \rightarrow [-\sigma, \sigma]^n$ for a vector.

In the position controlled tracking mode, the attitude dynamics is controlled to follow the computed attitude $R_c(t) \in \text{SO}(3)$ and the computed angular velocity $\Omega_c(t)$ defined as

$$R_c = [b_{1c}; b_{3c} \times b_{1c}; b_{3c}], \quad \hat{\Omega}_c = R_c^T \dot{R}_c, \quad (19)$$

¹see [19, Chapter 4] for the definition of partial stability

where $b_{3_c} \in S^2$ is given by

$$b_{3_c} = -\frac{-k_x e_x - k_v e_v - k_i \text{sat}_\sigma(e_i) - m g e_3 + m \ddot{x}_d}{\| -k_x e_x - k_v e_v - k_i \text{sat}_\sigma(e_i) - m g e_3 + m \ddot{x}_d \|}, \quad (20)$$

for positive constants k_x, k_v, k_i, σ . The unit vector $b_{1_c} \in S^2$ is selected to be orthogonal to b_{3_c} , thereby guaranteeing that $R_c \in \text{SO}(3)$. It can be chosen to specify the desired heading direction, and the detailed procedure to select b_{1_c} is described later at Section IV-C.

Following the prior definition of the attitude error and the angular velocity error, we define

$$e_R = \frac{1}{2}(R_c^T R - R^T R_c)^\vee, \quad e_\Omega = \Omega - R^T R_c \Omega_c, \quad (21)$$

and we also define the integral term of the attitude dynamics e_I as (14). It is assumed that

$$\| -k_x e_x - k_v e_v - k_i \text{sat}_\sigma(e_i) - m g e_3 + m \ddot{x}_d \| \neq 0, \quad (22)$$

and the commanded acceleration is uniformly bounded:

$$\| -m g e_3 + m \ddot{x}_d \| < B_1 \quad (23)$$

for a given positive constant B_1 . It is also assumed that an upper bound of the infinite norm of the uncertainty is known:

$$\| \Delta_x \|_\infty \leq \delta_x \quad (24)$$

for a given constant δ_x .

B. Position Tracking Controller

The nonlinear controller for the position controlled flight mode, described by control expressions for the thrust magnitude and the moment vector, are:

$$f = (k_x e_x + k_v e_v + k_i \text{sat}_\sigma(e_i) + m g e_3 - m \ddot{x}_d) \cdot R e_3, \quad (25)$$

$$M = -k_R e_R - k_\Omega e_\Omega - k_I e_I + (R^T R_c \Omega_c)^\wedge J R^T R_c \Omega_c + J R^T R_c \dot{\Omega}_c. \quad (26)$$

The nonlinear controller given by equations (25), (26) can be given a backstepping interpretation. The computed attitude R_c given in equation (19) is selected so that the thrust axis $-b_3$ of the quadrotor UAV tracks the computed direction given by $-b_{3_c}$ in (20), which is a direction of the thrust vector that achieves position tracking. The moment expression (26) causes the attitude of the quadrotor UAV to asymptotically track R_c and the thrust magnitude expression (25) achieves asymptotic position tracking. The saturation on the integral term is required to restrict the effects of the attitude tracking errors on the translational dynamics for the stability of the complete coupled system.

The corresponding closed loop control system is described by equations (1)-(4), using the controller expressions (25)-(26). We now state the result that the zero equilibrium of tracking errors $(e_x, e_v, e_R, e_\Omega)$ is exponentially stable.

Proposition 3: (Position Controlled Flight Mode) Suppose that the initial conditions satisfy

$$\Psi(R(0), R_c(0)) < \psi_1 < 1, \quad (27)$$

$$\|e_x(0)\| < e_{x_{\max}}, \quad (28)$$

for positive constants $\psi_1, e_{x_{\max}}$. Consider the control inputs f, M defined in (25)-(26). For positive constants k_x, k_v , we choose positive constants $c_1, c_2, k_R, k_\Omega, k_I, k_i, \sigma$ such that

$$k_i \sigma > \delta_x, \quad (29)$$

$$c_1 < \min \left\{ \frac{4k_x k_v (1 - \alpha)^2}{k_v^2 (1 + \alpha)^2 + 4mk_x (1 - \alpha)}, \sqrt{\frac{k_x}{m}} \right\}, \quad (30)$$

$$\lambda_m(W_2) > \frac{\|W_{12}\|^2}{4\lambda_m(W_1)}, \quad (31)$$

and (16) is satisfied, where $\alpha = \sqrt{\psi_1(2 - \psi_1)}$, and the matrices $W_1, W_{12}, W_2 \in \mathbb{R}^{2 \times 2}$ are given by

$$W_1 = \begin{bmatrix} c_1 k_x (1 - \alpha) & -\frac{c_1 k_v}{2} (1 + \alpha) \\ -\frac{c_1 k_v}{2} (1 + \alpha) & k_v (1 - \alpha) - m c_1 \end{bmatrix}, \quad (32)$$

$$W_{12} = \begin{bmatrix} c_1 (\sqrt{3} k_i \sigma + B_1) & 0 \\ k_i \sigma + B_1 + k_x e_{x_{\max}} & 0 \end{bmatrix}, \quad (33)$$

$$W_2 = \begin{bmatrix} c_2 k_R & -\frac{c_2}{2} (k_\Omega + B_2) \\ -\frac{c_2}{2} (k_\Omega + B_2) & k_\Omega - 2c_2 \lambda_M \end{bmatrix}. \quad (34)$$

Then, the zero equilibrium of the tracking errors is exponentially stable with respect to e_x, e_v, e_R, e_Ω , and the integral terms e_i, e_I are uniformly bounded.

Proof: See Appendix B. ■

Proposition 3 requires that the initial attitude error is less than 90° in (27). Suppose that this is not satisfied, i.e. $1 \leq \Psi(R(0), R_c(0)) < 2$. We can still apply Proposition 2, which states that the attitude error is asymptotically decreases to zero for almost all cases, and it satisfies (27) in a finite time. Therefore, by combining the results of Proposition 2 and 3, we can show attractiveness of the tracking errors when $\Psi(R(0), R_c(0)) < 2$.

Proposition 4: (Position Controlled Flight Mode with a Larger Initial Attitude Error) Suppose that the initial conditions satisfy

$$1 \leq \Psi(R(0), R_c(0)) < 2, \quad (35)$$

$$\|e_x(0)\| < e_{x_{\max}}, \quad (36)$$

for a constant $e_{x_{\max}}$. Consider the control inputs f, M defined in (25)-(26), where the control parameters satisfy (29)-(31) for a positive constant $\psi_1 < 1$. Then the zero equilibrium of the tracking errors is attractive, i.e., $e_x, e_v, e_R, e_\Omega \rightarrow 0$ as $t \rightarrow \infty$.

Proof: See Appendix C. ■

Linear or nonlinear PID controllers have been widely used for a quadrotor UAV. But, they have been applied in an *ad-hoc* manner without stability analysis. This paper provides a new form of nonlinear PID controller on SE(3) that guarantees almost global attractiveness in the presence of uncertainties. Compared with nonlinear robust control system [13], this paper yields stronger asymptotic stability without concern for chattering.

C. Direction of the First Body-Fixed Axis

As described above, the construction of the orthogonal matrix R_c involves having its third column b_{3_c} specified by (20), and its first column b_{1_c} is arbitrarily chosen to be orthogonal to the third column, which corresponds to a one-dimensional degree of choice.

By choosing b_{1_c} properly, we constrain the asymptotic direction of the first body-fixed axis. Here, we propose to specify the *projection* of the first body-fixed axis onto the plane normal to b_{3_c} . In particular, we choose a desired direction $b_{1_d} \in S^2$, that is not parallel to b_{3_c} , and b_{1_c} is selected as $b_{1_c} = \text{Proj}[b_{1_d}]$, where $\text{Proj}[\cdot]$ denotes the normalized projection onto the plane perpendicular to b_{3_c} . In this case, the first body-fixed axis does not converge to b_{1_d} , but it converges to the projection of b_{1_d} , i.e. $b_1 \rightarrow b_{1_c} = \text{Proj}[b_{1_d}]$ as $t \rightarrow \infty$. This can be used to specify the heading direction of a quadrotor UAV in the horizontal plane [23].

V. NUMERICAL EXAMPLE

The parameters of a quadrotor UAV are chosen as $J = [0.43, 0.43, 1.02] \times 10^{-2} \text{ kgm}^2$, $m = 0.755 \text{ kg}$, $d = 0.169 \text{ m}$, $c_{\tau f} = 0.0132 \text{ m}$. Disturbances for the translational dynamics and the rotational dynamics are chosen as

$$\Delta_x = [-0.5, 0.2, 1]^T \text{ N}, \quad \Delta_R = [0.2, -0.1, -0.02]^T \text{ Nm}.$$

Controller parameters are selected as follows: $k_x = 12.8$, $k_v = 4.22$, $k_i = 1.28$, $k_R = 0.65$, $k_\Omega = 0.11$, $k_I = 0.06$, $c_1 = 3.6$, $c_2 = 0.8$, $\sigma = 1$.

Initially, the quadrotor UAV is at a hovering condition: $x(0) = v(0) = \Omega(0) = 0_{3 \times 1}$, and $R(0) = I_{3 \times 3}$. The desired trajectory is a flipping maneuver where the quadrotor rotates about its second body-fixed axis by 360° , while changing the heading angle by 90° about the vertical e_3 axis. This is a complex maneuver combining a nontrivial pitching maneuver with a yawing motion. It is achieved by concatenating the following two control modes:

- (i) Attitude tracking to rotate the quadrotor ($t \leq 0.4$)

$$R_d(t) = \exp(\pi t \hat{e}_3) \exp(4\pi t \hat{e}_2).$$

- (ii) Trajectory tracking to make it hover after completing the preceding rotation ($0.4 < t \leq 4$)

$$x_d(t) = [0, 0, 0]^T, \quad b_{1_d} = [0, 1, 0]^T.$$

Figure 2 illustrate simulation results without the integral control terms proposed in this paper. There are steady state errors in attitude tracking and position tracking at Figures 2(a) and 2(b). The proposed integral control terms eliminate the steady state error while exhibiting good tracking performances as shown at Figure 3. The resulting controlled maneuver of the quadrotor UAV is illustrated at Figure 4.

In the prior results of generating nontrivial maneuvers of a quadrotor UAV, complicated reachability analyses are required to guarantee safe transitions between multiple control systems [15]. In the proposed geometric nonlinear control system, there are only two controlled flight modes for position tracking and attitude tracking, and each controller has

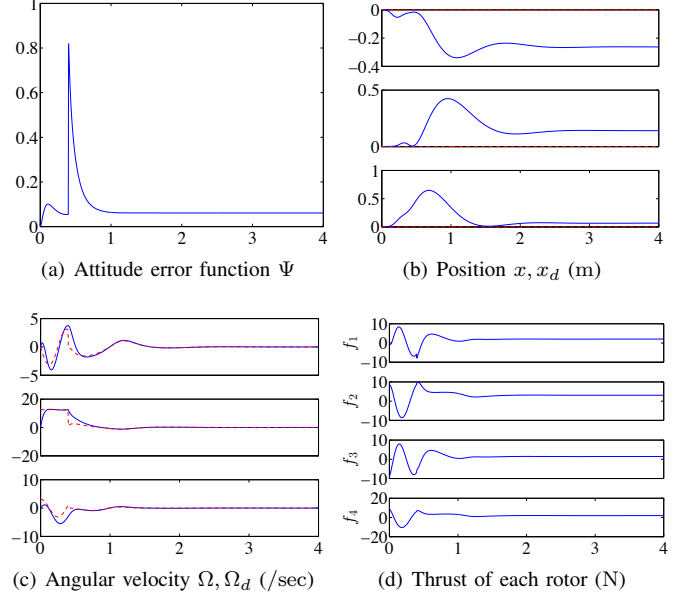


Fig. 2. Flipping without integral terms (red,dotted:desired, blue,solid:actual)

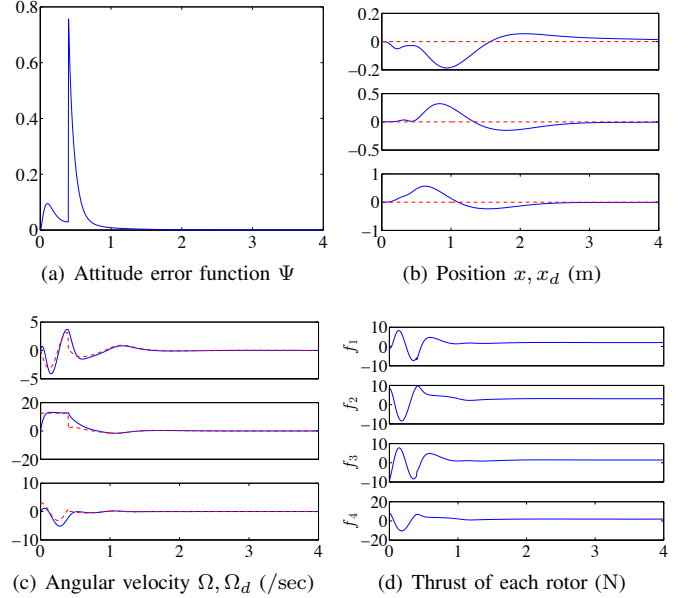


Fig. 3. Flipping with integral terms (red,dotted:desired, blue,solid:actual)

large region of attraction. Therefore, complex maneuvers can be easily generated in a unified way without need for time-consuming planning efforts, as illustrated by this numerical example. This is another unique contribution of this paper.

VI. PRELIMINARY EXPERIMENTAL RESULTS

Preliminary experimental results are provided for the attitude tracking control of a hardware system illustrated at Figure 5. To test the attitude dynamics, it is attached to a spherical joint. As the center of rotation is below the center of gravity, there exists a destabilizing gravitational moment, and the resulting attitude dynamics is similar to an inverted

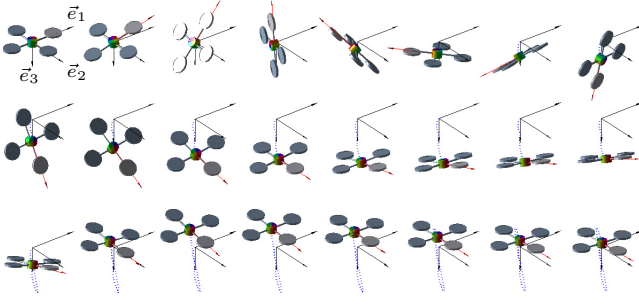


Fig. 4. Snapshots of a flipping maneuver with integral terms: the red axis denotes the direction of the first body-fixed axis. The quadrotor UAV rotates about the horizontal e_2 axis by 360° , while rotating its first body-fixed axis about the vertical e_3 axis by 90° . The trajectory of its mass center is denoted by blue, dotted lines.

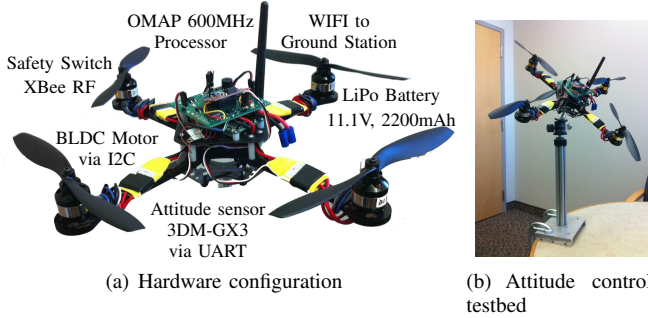


Fig. 5. Hardware development for a quadrotor UAV

rigid body pendulum. The control input at (13) is augmented with an additional term to eliminate the effects of the gravity.

The desired attitude command is described by using 3-2-1 Euler angles, i.e. $R_d(t) = R_d(\phi(t), \theta(t), \psi(t))$, where $\phi(t) = \frac{\pi}{9} \sin(\pi t)$, $\theta(t) = \frac{\pi}{9} \cos(\pi t)$, $\psi(t) = 0$. This represents a combined rolling and pitching motion with a period of 2 seconds. The results of the experiment are illustrated at Figure 6. This shows good tracking performances of the proposed control system in an experimental setting. Experiments for the position tracking is currently ongoing.

APPENDIX

A. Proof of Proposition 2

We first find the error dynamics for e_R, e_Ω , and define a Lyapunov function. Then, we find conditions on control parameters to guarantee the boundedness of tracking errors.

Using (3), (4), (26), the time-derivative of $J e_\Omega$ can be written as

$$J \dot{e}_\Omega = \{J e_\Omega + d\}^\wedge e_\Omega - k_R e_R - k_\Omega e_\Omega - k_I e_I + \Delta_R, \quad (37)$$

where $d = (2J - \text{tr}[J]I)R^T R_d \Omega_d \in \mathbb{R}^3$. The important property is that the first term of the right hand side is normal to e_Ω , and it simplifies the subsequent Lyapunov analysis.

Define a Lyapunov function \mathcal{V}_2 be

$$\begin{aligned} \mathcal{V}_2 = & \frac{1}{2} e_\Omega \cdot J e_\Omega + k_R \Psi(R, R_d) + c_2 e_R \cdot J e_\Omega \\ & + \frac{1}{2} k_I \|e_I - \frac{\Delta_R}{k_I}\|^2. \end{aligned} \quad (38)$$

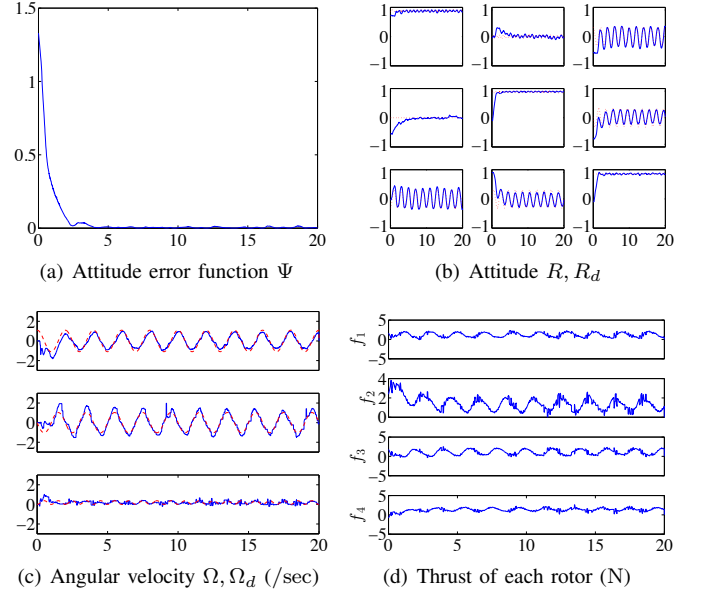


Fig. 6. Attitude tracking experiment (red,dotted:desired, blue,solid:actual)

From (10), (11), the Lyapunov function \mathcal{V}_2 is bounded as

$$\begin{aligned} z_2^T M_{21} z_2 + \frac{k_I}{2} \|e_I - \frac{\Delta_R}{k_I}\|^2 & \leq \mathcal{V}_2 \\ & \leq z_2^T M_{22} z_2 + \frac{k_I}{2} \|e_I - \frac{\Delta_R}{k_I}\|^2, \end{aligned} \quad (39)$$

where $z_2 = [\|e_R\|, \|e_\Omega\|]^T \in \mathbb{R}^2$, and the matrices M_{12}, M_{22} are given by

$$M_{21} = \frac{1}{2} \begin{bmatrix} k_R & -c_2 \lambda_M \\ -c_2 \lambda_M & \lambda_m \end{bmatrix}, \quad M_{22} = \frac{1}{2} \begin{bmatrix} \frac{2k_R}{2-\psi_2} & c_2 \lambda_M \\ c_2 \lambda_M & \lambda_M \end{bmatrix}. \quad (40)$$

From (11), the upper-bound of (39) is satisfied in the following domain:

$$D_2 = \{(R, \Omega) \in \text{SO}(3) \times \mathbb{R}^3 \mid \Psi(R, R_d) < \psi_2 < 2\}. \quad (41)$$

From (12), (37), the time derivative of \mathcal{V}_2 along the solution of the controlled system is given by

$$\begin{aligned} \dot{\mathcal{V}}_2 = & -k_\Omega \|e_\Omega\|^2 - e_\Omega \cdot (k_I e_I - \Delta_R) + c_2 \dot{e}_R \cdot J e_\Omega \\ & + c_2 e_R \cdot J \dot{e}_\Omega + (k_I e_I - \Delta_R) \dot{e}_I. \end{aligned}$$

From (14), we have $\dot{e}_I = c_2 e_R + e_\Omega$. Substituting this and (37), the above equation becomes

$$\begin{aligned} \dot{\mathcal{V}}_2 = & -k_\Omega \|e_\Omega\|^2 + c_2 \dot{e}_R \cdot J e_\Omega \\ & - c_2 k_R \|e_R\|^2 + c_2 e_R \cdot ((J e_\Omega + d)^\wedge e_\Omega - k_\Omega e_\Omega). \end{aligned}$$

Since $\|e_R\| \leq 1$, $\|\dot{e}_R\| \leq \|e_\Omega\|$, and $\|d\| \leq B_2$, we have

$$\dot{\mathcal{V}}_2 \leq -z_2^T W_2 z_2, \quad (42)$$

where the matrix $W_2 \in \mathbb{R}^{2 \times 2}$ is given by

$$W_2 = \begin{bmatrix} c_2 k_R & -\frac{c_2}{2} (k_\Omega + B_2) \\ -\frac{c_2}{2} (k_\Omega + B_2) & k_\Omega - 2c_2 \lambda_M \end{bmatrix}.$$

The condition on c_2 given at (16) guarantees that all of matrices M_{21}, W_2 are positive definite. This implies that the zero equilibrium of tracking errors $(e_R, e_\Omega, e_I) = (0, 0, \frac{\Delta_R}{k_I})$ is stable in the sense of Lyapunov, and $e_R, e_\Omega \rightarrow 0$ as $t \rightarrow \infty$. But, this does not necessarily implies $R \rightarrow R_d$ as $e_R = 0$ at any critical point of Ψ described at the property (iii) of Proposition 1.

Instead, we show instability of undesired equilibrium. Define $\mathcal{W}_2 = 2k_R - \mathcal{V}_2$. Then $\mathcal{W}_2 = 0$ at the undesired equilibria as $\Phi = 2$ at those points. Since

$$\mathcal{W}_2 \geq -\frac{\lambda_M}{2} \|e_\Omega\|^2 + k_R(2 - \Psi) - c_2 \|e_R\| \|e_\Omega\| - \frac{k_I}{2} \|e_I - \frac{\Delta_R}{k_I}\|^2.$$

Due to the continuity of Ψ , at any arbitrary small neighborhood of the undesired equilibrium attitude, we can choose R such that $2 - \Psi > 0$. Therefore, if $\|e_\Omega\|$ and $\|e_I - \frac{\Delta_R}{k_I}\|$ are sufficiently small, then $\mathcal{W}_2 > 0$ at such attitudes. In short, at any arbitrary small neighborhood of the undesired equilibrium, there exists a domain where $\mathcal{W}_2 > 0$, and $\dot{\mathcal{W}}_2 = -\dot{\mathcal{V}}_2 > 0$ in that domain from (42). According to Theorem 4.3 at [24], the undesired equilibrium is unstable.

The region of attraction to the desired equilibrium excludes the stable manifolds to the undesired equilibria. But the dimension of the union of the stable manifolds to the unstable equilibria is less than the tangent bundle of $SO(3)$. Therefore, the measure of the stable manifolds to the unstable equilibrium is zero. Then, the desired equilibrium is referred to as almost globally asymptotically stable with respect to e_R and e_Ω .

If this Lyapunov analysis is restricted to the domain D_2 , then the upper-bound of (39) is satisfied, and the condition on c_2 guarantees that the matrix M_{22} is positive definite. These yield local exponential stability with respect to e_R and e_Ω .

B. Proof of Proposition 3

We first derive the tracking error dynamics and a Lyapunov function for the translational dynamics of a quadrotor UAV, and later it is combined with the stability analyses of the rotational dynamics in Appendix A.

The subsequent analyses are developed in the domain D_1

$$D_1 = \{(e_x, e_v, R, e_\Omega) \in \mathbb{R}^3 \times \mathbb{R}^3 \times SO(3) \times \mathbb{R}^3 \mid \|e_x\| < e_{x_{\max}}, \Psi < \psi_1 < 1\}, \quad (43)$$

Similar to (11), we can show that

$$\frac{1}{2} \|e_R\|^2 \leq \Psi(R, R_c) \leq \frac{1}{2 - \psi_1} \|e_R\|^2. \quad (44)$$

a) *Translational Error Dynamics*: The time derivative of the position error is $\dot{e}_x = e_v$. The time-derivative of the velocity error is given by

$$m\dot{e}_v = m\ddot{x} - m\ddot{x}_d = mge_3 - fRe_3 - m\ddot{x}_d + \Delta_x. \quad (45)$$

Consider the quantity $e_3^T R_c^T Re_3$, which represents the cosine of the angle between $b_3 = Re_3$ and $b_{3_c} = R_c e_3$. Since $1 - \Psi(R, R_c)$ represents the cosine of the eigen-axis rotation

angle between R_c and R , we have $e_3^T R_c^T Re_3 \geq 1 - \Psi(R, R_c) > 0$ in D_1 . Therefore, the quantity $\frac{1}{e_3^T R_c^T Re_3}$ is well-defined. To rewrite the error dynamics of e_v in terms of the attitude error e_R , we add and subtract $\frac{f}{e_3^T R_c^T Re_3} R_c e_3$ to the right hand side of (45) to obtain

$$m\dot{e}_v = mge_3 - m\ddot{x}_d - \frac{f}{e_3^T R_c^T Re_3} R_c e_3 - X + \Delta_x, \quad (46)$$

where $X \in \mathbb{R}^3$ is defined by

$$X = \frac{f}{e_3^T R_c^T Re_3} ((e_3^T R_c^T Re_3) Re_3 - R_c e_3). \quad (47)$$

Let $A = -k_x e_x - k_v e_v - k_i \text{sat}_\sigma(e_i) - mge_3 + m\ddot{x}_d$. Then, from (20), (25), we have $b_{3_c} = R_c e_3 = -A / \|A\|$ and $f = -A \cdot Re_3$. By combining these, we obtain $f = (\|A\| R_c e_3) \cdot Re_3$. Therefore, the third term of the right hand side of (46) can be written as

$$-\frac{f}{e_3^T R_c^T Re_3} R_c e_3 = -\frac{(\|A\| R_c e_3) \cdot Re_3}{e_3^T R_c^T Re_3} \cdot \frac{A}{\|A\|} = A = -k_x e_x - k_v e_v - k_i \text{sat}_\sigma(e_i) - mge_3 + m\ddot{x}_d.$$

Substituting this into (46), the error dynamics of e_v can be written as

$$m\dot{e}_v = -k_x e_x - k_v e_v - k_i \text{sat}_\sigma(e_i) - X + \Delta_x. \quad (48)$$

b) *Lyapunov Candidate for Translation Dynamics*: Let a Lyapunov candidate \mathcal{V}_1 be

$$\mathcal{V}_1 = \frac{1}{2} k_x \|e_x\|^2 + \frac{1}{2} m \|e_v\|^2 + c_1 e_x \cdot m e_v + \int_{\frac{\Delta_x}{k_i}}^{e_i} (k_i \text{sat}_\sigma(\mu) - \Delta_x) \cdot d\mu. \quad (49)$$

The condition given at (29) implies that the last integral term of the above equation is positive definite about $e_i = \frac{\Delta_x}{k_i}$. The derivative of \mathcal{V}_1 along the solution of (48) is given by

$$\dot{\mathcal{V}}_1 = -(k_v - mc_1) \|e_v\|^2 - c_1 k_x \|e_x\|^2 - c_1 k_v e_x \cdot e_v + X \cdot \{c_1 e_x + e_v\}. \quad (50)$$

The last term of the above equation corresponds to the effects of the attitude tracking error on the translational dynamics. We find a bound of X , defined at (47), to show stability of the coupled translational dynamics and rotational dynamics in the subsequent Lyapunov analysis. Since $f = \|A\| (e_3^T R_c^T Re_3)$, we have

$$\begin{aligned} \|X\| &\leq \|A\| \|(e_3^T R_c^T Re_3) Re_3 - R_c e_3\| \\ &\leq (k_x \|e_x\| + k_v \|e_v\| + \sqrt{3} k_i \sigma + B_1) \\ &\quad \times \|(e_3^T R_c^T Re_3) Re_3 - R_c e_3\|. \end{aligned}$$

The last term $\|(e_3^T R_c^T Re_3) Re_3 - R_c e_3\|$ represents the sine of the angle between $b_3 = Re_3$ and $b_{3_c} = R_c e_3$, since $(b_{3_c} \cdot b_3) b_3 - b_{3_c} = b_3 \times (b_3 \times b_{3_c})$. The magnitude of the attitude error vector, $\|e_R\|$ represents the sine of the eigen-axis rotation angle between R_c and R (see [23]). Therefore, $\|(e_3^T R_c^T Re_3) Re_3 - R_c e_3\| \leq \|e_R\|$ in D_1 . It follows that

$$\|(e_3^T R_c^T Re_3) Re_3 - R_c e_3\| \leq \|e_R\| = \sqrt{\Psi(2 - \Psi)}$$

$$\leq \left\{ \sqrt{\psi_1(2-\psi_1)} \triangleq \alpha \right\} < 1. \quad (51)$$

Therefore, X is bounded by

$$\begin{aligned} \|X\| &\leq (k_x \|e_x\| + k_v \|e_v\| + \sqrt{3}k_i \sigma + B_1) \|e_R\| \\ &\leq (k_x \|e_x\| + k_v \|e_v\| + \sqrt{3}k_i \sigma + B_1) \alpha. \end{aligned} \quad (52)$$

Substituting (52) into (50),

$$\begin{aligned} \dot{\mathcal{V}}_1 &\leq -(k_v(1-\alpha) - mc_1) \|e_v\|^2 - c_1 k_x (1-\alpha) \|e_x\|^2 \\ &\quad + c_1 k_v (1+\alpha) \|e_x\| \|e_v\| \\ &\quad + \|e_R\| \left\{ (\sqrt{3}k_i \sigma + B_1)(c_1 \|e_x\| + \|e_v\|) + k_x \|e_x\| \|e_v\| \right\}. \end{aligned} \quad (53)$$

In the above expression for $\dot{\mathcal{V}}_1$, there is a third-order error term, namely $k_x \|e_R\| \|e_x\| \|e_v\|$. Using (51), it is possible to choose its upper bound as $k_x \alpha \|e_x\| \|e_v\|$ similar to other terms, but the corresponding stability analysis becomes complicated, and the initial attitude error should be reduced further. Instead, we restrict our analysis to the domain D_1 defined in (43), and its upper bound is chosen as $k_x e_{x_{\max}} \|e_R\| \|e_v\|$.

c) *Lyapunov Candidate for the Complete System:* Let $\mathcal{V} = \mathcal{V}_1 + \mathcal{V}_2$ be the Lyapunov candidate of the complete system. Define $z_1 = [\|e_x\|, \|e_v\|]^T$, $z_2 = [\|e_R\|, \|e_\Omega\|]^T \in \mathbb{R}^2$, and

$$\mathcal{V}_I = k_i \int_{\frac{\Delta_x}{k_i}}^{e_i} (\text{sat}_\sigma(\mu) - \Delta_x) \cdot d\mu + \frac{k_I}{2} \|e_I - \frac{\Delta_R}{k_I}\|^2.$$

Using (44), the bound of the Lyapunov candidate \mathcal{V} can be written as

$$\begin{aligned} z_1^T M_{11} z_1 + z_2^T M_{21} z_2 + \mathcal{V}_I &\leq \mathcal{V} \\ &\leq z_1^T M_{12} z_1 + z_2^T M'_{22} z_2 + \mathcal{V}_I, \end{aligned} \quad (54)$$

where the matrices $M_{11}, M_{12}, M_{21}, M_{22}$ are given by

$$\begin{aligned} M_{11} &= \frac{1}{2} \begin{bmatrix} k_x & -mc_1 \\ -mc_1 & m \end{bmatrix}, \quad M_{12} = \frac{1}{2} \begin{bmatrix} k_x & mc_1 \\ mc_1 & m \end{bmatrix}, \\ M_{21} &= \frac{1}{2} \begin{bmatrix} k_R & -c_2 \lambda_M \\ -c_2 \lambda_M & \lambda_m \end{bmatrix}, \quad M'_{22} = \frac{1}{2} \begin{bmatrix} \frac{2k_R}{2-\psi_1} & c_2 \lambda_M \\ c_2 \lambda_M & \lambda_M \end{bmatrix}. \end{aligned}$$

Using (42) and (53), the time-derivative of \mathcal{V} is given by

$$\dot{\mathcal{V}} \leq -z_1^T W_1 z_1 + z_1^T W_{12} z_2 - z_2^T W_2 z_2 \leq -z^T W z \quad (55)$$

where $z = [z_1, z_2]^T \in \mathbb{R}^2$, and the matrices $W_1, W_{12}, W_2 \in \mathbb{R}^{2 \times 2}$ are defined at (32)-(34). The matrix $W \in \mathbb{R}^{2 \times 2}$ is given by

$$W = \begin{bmatrix} \lambda_m(W_1) & -\frac{1}{2} \|W_{12}\|_2 \\ -\frac{1}{2} \|W_{12}\|_2 & \lambda_m(W_2) \end{bmatrix}.$$

The conditions given at (16), (30), (31) guarantee that all of matrices $M_{11}, M_{21}, M_{21}, M'_{22}, W$ are positive definite, and (29) implies that the integral term of \mathcal{V}_1 at (49) is positive definite about $e_i = \frac{\Delta_x}{k_i}$. This implies that the zero equilibrium of the tracking error is exponentially stable with respect to e_x, e_v, e_R, e_Ω , and the integral terms e_i, e_I are uniformly bounded.

C. Proof of Proposition 4

According to the proof of Proposition 2, the attitude tracking errors asymptotically decrease to zero, and therefore, they enter the region given by (27) in a finite time t^* , after which the results of Proposition 3 can be applied to yield attractiveness. The remaining part of the proof is showing that the tracking error $z_1 = [\|e_x\|, \|e_v\|]^T$ is bounded in $t \in [0, t^*]$. This is similar to the proof given at [25], [26].

REFERENCES

- [1] S. Bouabdalla and R. Siegward, "Backstepping and sliding-mode techniques applied to an indoor micro quadrotor," in *Proceedings of the IEEE International Conference on Robotics and Automation*, 2005, pp. 2259–2264.
- [2] M. Efe, "Robust low altitude behavior control of a quadrotor rotorcraft through sliding modes," in *Proceedings of the Mediterranean Conference on Control and Automation*, 2007.
- [3] C. Nicol, C. Macnab, and A. Ramirez-Serrano, "Robust neural network control of a quadrotor helicopter," in *Proceedings of the Canadian Conference on Electrical and Computer Engineering*, 2008, pp. 1233–1237.
- [4] D. Mellinger, N. Michael, and V. Kumar, "Trajectory generation and control for precise aggressive maneuvers with quadrotors," *International Journal Of Robotics Research*, vol. 31, no. 5, pp. 664–674, 2012.
- [5] A. Tayebi and S. McGilvray, "Attitude stabilization of a VTOL quadrotor aircraft," *IEEE Transactions on Control System Technology*, vol. 14, no. 3, pp. 562–571, 2006.
- [6] S. Bhat and D. Bernstein, "A topological obstruction to continuous global stabilization of rotational motion and the unwinding phenomenon," *Systems and Control Letters*, vol. 39, no. 1, pp. 66–73, 2000.
- [7] C. Mayhew, R. Sanfelice, and A. Teel, "Quaternion-based hybrid control for robust global attitude tracking," *IEEE Transactions on Automatic Control*, vol. 56, no. 11, pp. 2555–2566, 2011.
- [8] D. Cabecinhas, R. Cunha, and C. Silvestre, "Rotorcraft path following control for extended flight envelope coverage," in *Proceedings of the IEEE Conference on Decision and Control*, 2009, pp. 3460–3465.
- [9] D. Mellinger and V. Kumar, "Minimum snap trajectory generation and control for quadrotors," in *Proceedings of the International Conference on Robotics and Automation*, 2011.
- [10] R. Naldi, L. Marconi, and L. Gentili, "Robust takeoff and landing for a class of aerial robots," in *Proceedings of the IEEE Conference on Decision and Control*, 2009, pp. 3436–3441.
- [11] M. Hua, T. Hamel, P. Morin, and C. Samson, "A control approach for thrust-propelled underactuated vehicles and its application to VTOL drones," *IEEE Transactions on Automatic Control*, vol. 54, no. 8, pp. 1834–1853, 2009.
- [12] T. Lee, M. Leok, and N. McClamroch, "Geometric tracking control of a quadrotor UAV on SE(3)," in *Proceedings of the IEEE Conference on Decision and Control*, 2010, pp. 5420–5425.
- [13] —, "Nonlinear robust tracking control of a quadrotor UAV on SE(3)," in *Proceeding of the American Control Conference*, 2012, pp. 4649–4654.
- [14] N. Chaturvedi, A. Sanyal, and N. McClamroch, "Rigid-body attitude control," *IEEE Control Systems Magazine*, vol. 31, no. 3, pp. 30–51, 2011.
- [15] J. Gillula, G. Hoffmann, H. Huang, M. Vitus, and C. Tomlin, "Applications of hybrid reachability analysis to robotic aerial vehicles," *The International Journal of Robotics Research*, vol. 30, no. 3, pp. 335–354, 2011.
- [16] P. Castillo, R. Lozano, and A. Dzul, "Stabilization of a mini rotorcraft with four rotors," *IEEE Control System Magazine*, pp. 45–55, 2005.
- [17] F. Bullo and A. Lewis, *Geometric control of mechanical systems*, ser. Texts in Applied Mathematics. New York: Springer-Verlag, 2005, vol. 49, modeling, analysis, and design for simple mechanical control systems.
- [18] T. Lee, "Robust adaptive geometric tracking controls on SO(3) with an application to the attitude dynamics of a quadrotor UAV," arXiv, 2011. [Online]. Available: <http://arxiv.org/abs/1108.6031>

- [19] W. Haddad and V. Chellaboina, *Nonlinear Dynamical Systems and Control: A Lyapunov-Based Approach*. Princeton University Press, 2008.
- [20] K. Subbarao, "Nonlinear PID-like controllers for rigid-body attitude stabilization," *Journal of the Astronautical Sciences*, vol. 52, no. 1-2, pp. 61–74, 2004.
- [21] K. Subbarao and M. Akella, "Differentiator-free nonlinear proportional-integral controllers for rigid-body attitude stabilization," *Journal of Guidance, Control, and Dynamics*, vol. 27, no. 6, pp. 1092–1096, 2004.
- [22] L. Show, J. Juang, C. Lin, and Y. Jan, "Spacecraft robust attitude tracking design: PID control approach," in *Proceeding of the American Control Conference*, 1360-1365, Ed., 2002.
- [23] T. Lee, M. Leok, and N. McClamroch, "Control of complex maneuvers for a quadrotor UAV using geometric methods on $SE(3)$," arXiv. [Online]. Available: <http://arxiv.org/abs/1003.2005>
- [24] H. Khalil, *Nonlinear Systems*. Prentice Hall, 2002.
- [25] T. Lee, M. Leok, and N. McClamroch, "Nonlinear robust tracking control of a quadrotor UAV on $SE(3)$," arXiv. [Online]. Available: <http://arxiv.org/abs/1109.4457>
- [26] —, "Nonlinear robust tracking control of a quadrotor UAV on $SE(3)$," *Asian Journal of Control*, 2012, accepted.